Energy Storage Materials 23 (2019) 427–433

Contents lists available at ScienceDirect

Energy Storage Materials

journal homepage: www.elsevier.com/locate/ensm

In operando formation of new iron-oxyfluoride host structure for Na-ion storage from NaF–FeO nanocomposite

Insang Hwang [a], Sung-Kyun Jung [a], Sung-Pyo Cho [b], Kisuk Kang [a,c,*]

[a] Department of Materials Science and Engineering, Research Institute of Advanced Materials (RIAM), Seoul National University, Seoul 08826, Republic of Korea
[b] National Center for Inter-University Research Facilities, Seoul National University, Seoul 08826, Republic of Korea
[c] Center for Nanoparticle Research, Institute for Basic Science (IBS), Seoul National University, Seoul 08826, Republic of Korea

A B S T R A C T

Herein, we report a cubic FeOF structure as a new reversible Na ion host, which is formed during the electrochemical reaction from an electrode based on a nanosized mixture of NaF and FeO. This new FeOF host structure differs from the well-known rutile FeOF structure and displays distinct electrochemical properties as an electrode for Na-ion batteries. The X-ray absorption spectra measured at various cycles indicate that the cubic FeOF host structure gradually forms as cycling progresses. After formation of the cubic FeOF host structure, a discharge capacity of 165 mAh/g is delivered, corresponding to the intercalation of 0.7 Na^+ ions per Fe with a volume change of 2.3% during charge and discharge, which is offered at a higher redox potential than that of the rutile FeOF electrode by approximately 0.2 V.

Na-ion batteries (NIBs) have attracted considerable attention as an alternative to Li-ion batteries (LIBs) because their components are more abundant in nature and more cost-effective than those of LIBs. The key to the success of NIBs lies in discovering new electrode materials that can provide high energy density. However, the search for new Na-ion host structures has been challenging because of the limited number of host crystalline materials in which Na de/intercalation can reversibly occur [1–4]. For the past decades, extensive research has led to the identification of important NIB cathode materials, including layered-type O3-$NaTMO_2$ (TM = Co, Mn, Cr, Fe, and Ni) [5–10], P2-$Na_x(Fe, Mn)O_2$ ($0 < x < 1$) [11–14], and polyanionic compounds such as $Na_3(VO_x)_2(PO_4)_2F_{2-2x}$ ($0 < x < 1$) [15–17] and $NaFeSO_4F$ [18–20]. Although these materials show promising electrochemical performance, the energy densities that they are capable of delivering do not yet reach those of state-of-the-art electrode materials in LIBs.

Recently, a new approach for cathode material design involving nanoscale mixing of alkali (Li or Na) metal compounds and transition metal compounds was reported [21–31]. In nanocomposite electrodes, the initial electrochemical reaction occurs via the extraction of ions from the alkali metal compounds and electrons from the transition metal compounds. Thus, the two compounds in the nanocomposite serve as an ion host and an electron host, respectively. The concept is similar to the 'job-sharing' mechanism observed at the nanoscale interface proposed by Maier et al. in that two different hosts share the electrochemical reaction but differs in that the anion from the alkali metal compounds mediate the reaction; thus, the whole bulk structural materials can participate in the reaction [32,33]. These types of nanocomposite electrode reactions are generally activated by the initial charge process, which is the decomposition reaction of alkali metal compounds such as LiF and NaF [23,24]. During the charge process, the liberated F^- ion (the decomposition product of the alkali metal compounds) is absorbed on and/or diffuses into the transition metal compounds and activates the nanocomposite electrodes [21–24,26,27]. Although reports on nanocomposite electrodes are limited and further understanding is needed, the nanocomposite electrodes have been reported to follow one of two reaction mechanisms: 'surface conversion' or 'host formation'. In the materials that follow the 'surface conversion' reaction, the reaction mainly occurs at the surface of the transition metal compounds, accompanying the phase transformation at the surface (*e.g.,* LiF–MnO) [21]. For the 'host formation' reaction, new host structures for the respective alkali ions are formed during charge, and further reaction occurs via intercalation/deintercalation of alkali ions in the host structure. It has been reported that intercalation hosts could form, such as FeF_3 from LiF–FeF_2 [23] and NaF–FeF_2 [24] nanocomposite reactions, $LiFeSO_4F$ from LiF–$FeSO_4$ [29], and $Li_3(VPO_4)_2F_3$ from 3LiF–$2VPO_4$ [31], all of which were previously well-known host crystalline structures for either Li or Na. More recently, it was also observed that the host formation reaction can lead to the formation of new host structure, which has not been observed before. Jung et al. showed that for the LiF–FeO nanocomposite, a cubic FeOF structure was unexpectedly formed with the same

* Corresponding author. Department of Materials Science and Engineering, Research Institute of Advanced Materials (RIAM), Seoul National University, Seoul 08826, Republic of Korea.
E-mail address: matlgen1@snu.ac.kr (K. Kang).

https://doi.org/10.1016/j.ensm.2019.04.020
Received 12 January 2019; Received in revised form 16 April 2019; Accepted 17 April 2019
Available online 26 April 2019

composition as the well-known rutile FeOF structure but with a different crystalline symmetry [22]. This finding implies that the utilization of the host formation reaction can be an interesting new approach to explore cathode materials with new intercalation host structures.

Here, we report a novel host structure for Na-ion storage, a cubic polymorph of the FeOF structure from a 'host formation' reaction, and reveal that this structure can serve as a promising new electrode material for NIBs with a respectable energy density and can outperform well-known rutile FeOF electrodes. The NaF–FeO nanocomposite was prepared by mixing NaF and FeO powder using high-energy ball milling. An X-ray diffraction (XRD) pattern of the as-synthesized NaF–FeO nanocomposite is presented in Fig. 1 (a). Only peaks originating from NaF and FeO are observed in the XRD pattern, indicating that no side reactions or phase transformations occurred during the ball milling. The broad peaks in the XRD pattern suggest the size reduction of the NaF and FeO crystalline phases after the ball milling. The retention of each phase after ball milling was also confirmed by transmission electron microscopy (TEM) diffraction pattern (DP) analysis (Fig. S1). The *d*-spacings in the DP image agree well with those of NaF and FeO, and the hollow-ring pattern with some bright spots indicates the random orientation of each crystalline phase in the nanocomposite. The scanning electron microscopy (SEM) images in Fig. S2 reveal that the pristine NaF and FeO particles with sizes of tens of micrometers were broken down into smaller pieces after the ball milling with average crystalline sizes of approximately 10 nm according to Williamson–Hall plots (Fig. S3).

Fig. 1 (b) presents the first charge and discharge profiles of the NaF–FeO nanocomposite electrode in a Na half-cell configuration with metallic Na as the anode and 1 M $NaPF_6$ in ethylene carbonate/propylene carbonate (EC/PC, 1/1, v/v) as the electrolyte in the voltage window of 1.2–4.4 V (*vs.* Na^+/Na) using a current density of 50 mA/g at 60 °C. The NaF–FeO nanocomposite electrode could deliver a discharge capacity of 150 mAh/g after the initial charging to 4.4 V, corresponding to the reaction of 0.6 Na ion per transition metal ion. The origin of the reversible capacity was probed using X-ray absorption near edge spectroscopy (XANES) at the Fe K-edge (Fig. 1 (c)). In the XANES spectra, the Fe K-edge shifts to higher energy during charge and shifts back to lower energy during discharge, which indicates the reversible oxidation and reduction of Fe during the electrochemical reactions. The F K-edge X-ray absorption spectroscopy (XAS) spectra in Fig. 1 (d) and (e) demonstrate that F^- anion incorporation to FeO occurs during charge process, which is consistent with the previous observations of the F anion mediation in the nanocomposite electrochemical reaction [21–24]. The F K-edge XAS spectra were simultaneously recorded in total fluorescence yield (TFY) and total electron yield (TEY) modes. Note that the surface-sensitive TEY mode collects signals from the near surface (~5–10 nm), whereas the TFY mode is more bulk sensitive. The NaF signals in the F K-edge region are broadly located from 688 to 700 eV with two characteristic peaks in the pristine NaF–FeO nanocomposite [34–36]. During charge, these signals from NaF decreased with a notable reduction in the peak at ~700 eV, and a new peak at 684 eV arose in both the TFY and TEY modes. The signal at 684.3 eV is attributed to F–Fe bonding, which originates from hybridization between Fe 3*d* and F 2*p* orbitals, whereas the peak denoted by * is generated by energy absorption from F in both the Fe–F and NaF [34,37–39]. These results suggest that decomposition of NaF occurred during charge and that the liberated F was absorbed on the FeO to form Fe–F bonding, similar to the behavior observed for a LiF–FeO nanocomposite electrode in a Li cell [22]. Clear evidence of the NaF decomposition during charge was also observed in the *ex situ* XRD analysis, as presented in Fig. S4.

The electrochemical performance of the NaF–FeO nanocomposite electrode was further investigated with cycles in Fig. 2 (a). Notably, the charge/discharge profiles of the nanocomposite electrode gradually

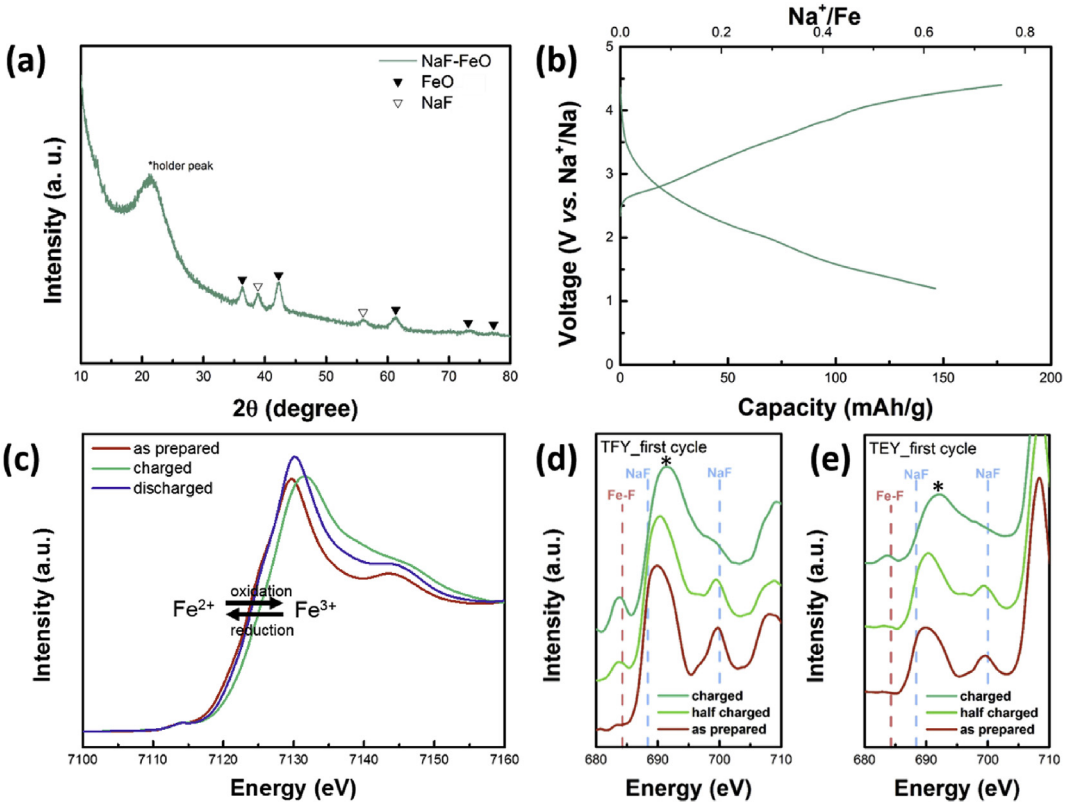

Fig. 1. **(a)** XRD pattern of as-prepared NaF–FeO nanocomposite powder. **(b)** First charge/discharge profiles of NaF–FeO nanocomposite electrode at current density of 50 mA/g at 60 °C. **(c)** Fe K-edge XANES spectra and F K-edge XAS spectra in **(d)** bulk-sensitive TFY mode and **(e)** surface-sensitive TEY mode in the first cycle. The red and blue dotted lines in Fig. 1 (d) and (e) represent the characteristic F K-edge spectrum of Fe–F bonding and NaF. The peak marked with * is the main peak generated by energy absorption from F in both the Fe–F and NaF.

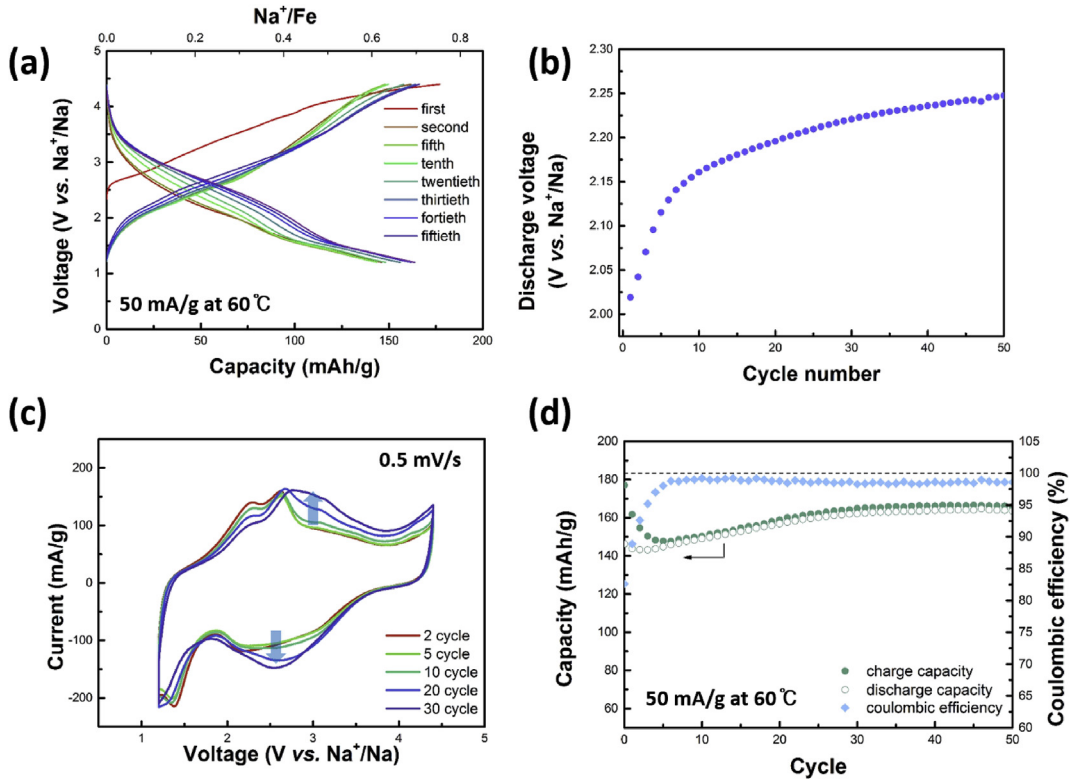

Fig. 2. **(a)** Charge/discharge profiles of NaF–FeO nanocomposite for the first 50 cycles. **(b)** Average discharge voltage as a function of cycle number. **(c)** CV profiles at various cycles at scan rate of 0.5 mV/s. **(d)** Cycle life and coulombic efficiency of NaF–FeO nanocomposite at current density of 50 mA/g.

changed as cycling proceeded. For the initial discharge, a sloping profile was observed (Fig. 1 (b)), whereas the discharge profile after 50 cycles increasingly displayed a plateau-like region at approximately 2.5 V. Quantitative examination of the average discharge voltage in Fig. 2 (b) confirms the increase from 2.0 V in the 1st cycle to 2.25 V in the 50th cycle. The change in the redox potential was also evident in the cyclic voltammetry (CV) measurements (Fig. 2 (c)) and dQ/dV analysis (Fig. S5) for different cycles, which show that the peak at ~2.5 V progressively emerged as cycling progressed. With the emergence of the plateau region, the discharge capacity also increased from 150 mAh/g in the 1st cycle to 165 mAh/g in the 50th cycle (Fig. 2 (d)). The evolution of the plateau-like region implies that substantial amounts of Na ions are stored in the local environments with equivalent Na chemical potentials, which is hardly observed for the surface or capacitive electrochemical reactions. In addition, the increase in the discharge voltage indicates the formation of energetically more stable storage sites for Na ions from the NaF–FeO nanocomposite electrode as cycling progresses. Both features strongly suggest the gradual formation of the host structure for Na ions evolving from the NaF–FeO nanocomposite.

From the initial stoichiometry of the NaF–FeO nanocomposite and the fact that NaF decomposes and Fe–F bonding is formed during charging, the host structure formed is likely to be iron oxyfluoride (FeOF). However, it is noted that the discharge voltage of the iron oxyfluoride observed here is substantially higher than that of the well-known rutile FeO_xF_{2-x} ($0 < x \leq 1$). In our case, almost half of the capacity was delivered above 2.5 V after the formation of the host structure, whereas, according to previous studies, negligible capacity could be delivered above 2.5 V for rutile FeO_xF_{2-x} ($0 < x \leq 1$) electrodes [40–42]. This difference suggests that the host structure formed during electrochemical charge/-discharge of NaF–FeO may differ from the rutile FeO_xF_{2-x} ($0 < x \leq 1$) structure. To gain further insight into the host structure, *ex situ* XRD analysis was performed, as shown in Fig. 3 (a). In this figure, the number corresponds to the cycle number, and C and D indicate the charged and discharged state, respectively. In the as-prepared state, the characteristic (111), (200), and (220) peaks of FeO were clearly observed at 36.4°, 42.3°, and 61.4°. However, after 5 electrochemical cycles, the peaks from FeO decreased, and new peaks began to emerge at 35.2°, 43.0°, and 62.5°; after 20 cycles, these peaks were dominant over the pristine FeO peaks (Fig. S6). The new peaks generally match with those of Fe_2O_3 with cubic $P4_132$ symmetry, where the anion is richer than the cation, implying that the iron oxyfluoride that is likely to be formed resembles the crystal structure of cubic Fe_2O_3. The one of the possible reason why iron oxyfluoride formed in NaF-FeO shows an XRD pattern similar to that of cubic Fe_2O_3 is that the atomic arrangement iron oxyfluoride formed in NaF-FeO is similar to that of cubic Fe_2O_3, and the atomic numbers of F and O are similar, which makes it difficult to distinguish them on XRD.

We attempted to directly visualize the crystalline structure of the new host using Cs-corrected high-angle annular dark-field scanning transmission electron microscopy (HAADF-STEM), as shown in Fig. 3 (b). The atomic arrangement different from that of FeO was observed throughout the particle and the fast Fourier transform (FFT) image of the sample in the inset of Fig. 3 (b) shows characteristic spots at 0.217 nm (blue), 0.261 nm (green), and 0.439 nm (yellow), which do not match with those of the pristine rocksalt FeO structure. The detailed structure was further probed in the area enclosed by the green box using atomic-resolution HAADF-STEM, as shown in Fig. 3 (c). The results consistently indicate that the new host differs from the pristine FeO. The atomic arrangement shown in Fig. 3 (c) matched well with the characteristic Fe arrangement in the (110) plane of cubic Fe_2O_3, which agrees with the *ex situ* XRD analysis in Fig. 3 (a). The line intensity profile alternates between a relatively dark spot (red) and a bright spot (green), and the dissimilar intensities of the red and green spots suggest the different number of atoms present in each column. It is noteworthy that the number of atoms in the green column is almost twice that in the red column in a typical cubic Fe_2O_3 structure, unlike in the rocksalt structure.

The HAADF-STEM and *ex situ* XRD analyses suggest that the host structure has cubic symmetry with Fe atomic arrangement similar to that of cubic Fe_2O_3. Given that the initial Fe:O stoichiometry is 1:1 and that

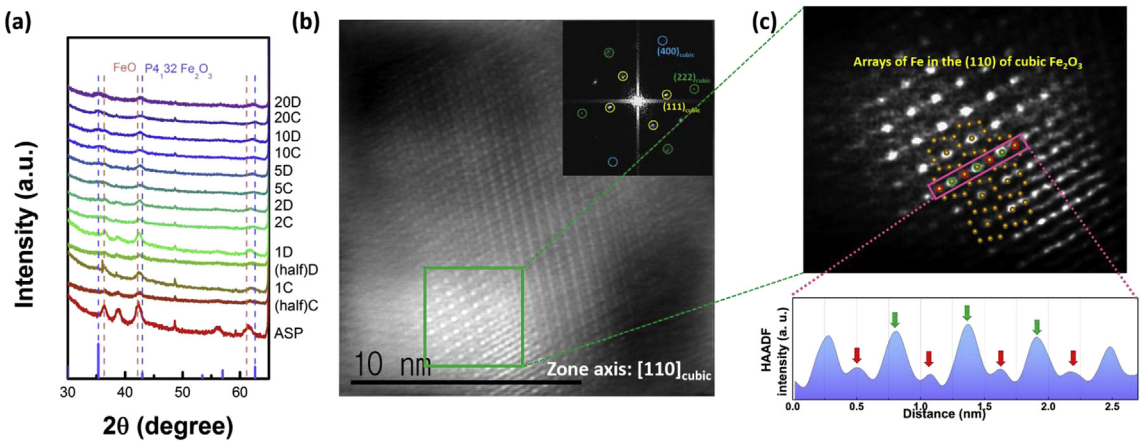

Fig. 3. **(a)** *Ex situ* XRD patterns of NaF–FeO nanocomposite electrodes. The red dotted lines indicate the peak positions of cubic FeO, and the purple dotted lines indicate the peak positions of cubic Fe_2O_3. **(b)** HAADF-STEM image of 20th discharged electrode (inset: FFT image). **(c)** Fe atomic arrangement of the area enclosed by the green box in (b). The Fe atomic arrangement of the (110) plane of cubic Fe_2O_3 is also shown. HAADF line intensity profile measured in the area enclosed by the black box. The red arrows indicate relatively dark spots, and the green arrows indicate relatively bright spots.

the oxidation state of Fe increases close to +3, we suspect that the host structure formed in the NaF–FeO nanocomposite electrode is FeOF with cubic symmetry. The formation of cubic FeOF was also recently reported in the electrochemical cycling of a LiF–FeO nanocomposite electrode operated in a Li cell, which served as a Li intercalation host [22]. The DFT calculation performed in LiF-FeO work showed that the formation energy of cubic FeOF is 26.6 meV/f.u. higher than that of rutile FeOF which showed feasibility of forming cubic FeOF as metastable phase. The formation of cubic FeOF in both LiF–FeO and NaF–FeO systems implies that the formation of cubic FeOF might be a universal phenomenon if appropriate F-donating sources, such as LiF and NaF, are supplied. Moreover, the fact that cubic FeOF is formed instead of the thermodynamically stable rutile FeOF suggests that the initial crystalline symmetry of the pristine FeO has guided the formation of the cubic FeOF. The electrochemical reaction occurs at a relatively low temperature compared with the synthesis temperature of iron oxyfluorides, which is typically above 300 °C [40,43]. The low temperature during the phase transformation may lead to the sluggish atomic diffusion in the NaF–FeO nanocomposite, trapping it in the metastable cubic FeOF phase and retaining the pristine symmetry of FeO. After the formation of the host structure, the lattice parameter was 8.377 Å in the charged state and 8.440 Å in the discharged state within the cubic symmetry (Fig. S7) [22]. Thus, the volume change during charge and discharge was 2.3%, which is slightly larger than the volume change of 1.5% for cubic FeOF operated in a Li cell system [22]. The larger volume change in the Na system than in the Li system may be attributed to the larger radius of Na ions than Li ions in the intercalation.

To attain a better understanding of the formation mechanism of the host structure, *ex situ* F K-edge XAS analysis was performed as cycling progressed (Fig. 4). Fig. 4 (a) and (b) show that, in the charged state, the signals from NaF were barely detected, whereas signals from Fe–F bonding were observed both in the bulk (TFY mode) and at the surface (TEY mode) for all the cycles. These findings indicate that F binds with Fe in FeO not only at the surface but also within the bulk in the charged states regardless of the cycle number. The Fe K-edge EXAFS spectra in the charged state also indicate that the changes in the EXAFS for different cycles were relatively small, suggesting that the local environment around Fe in the charged state was similar for all the cycles after the first charge process (Fig. 4 (c)). However, in the discharged state, comparatively different XAS signals were observed for the bulk (Fig. 4 (d)) and surface (Fig. 4 (e)). For the initial few discharged cycle states (1D and 2D), the Fe–F bonding signal was only detectable in the bulk (*i.e.,* TFY mode), whereas the NaF signal was detected for both modes. The XAS results suggest that most of the Na ions could not intercalate into the FeOF structure and underwent a surface conversion reaction to form NaF at the surface, similar to the findings in the LiF–MnO nanocomposite after the first discharge [21], whereas a fraction of FeOF could be retained in the bulk, allowing Na-ion intercalation. As cycling proceeded, the Fe–F signal began to emerge in the surface-sensitive TEY mode and the NaF signals were gradually reduced in both the TFY and TEY modes in the discharged state. These results imply that the phase transition propagates from the bulk to the surface and that the NaF formation becomes difficult even at the surface, most likely because of the completion of the formation of the host structure. This gradual change in the discharged state was also confirmed by the Fe K-edge EXAFS results, as shown in Fig. 4 (f). In this figure, the peak at 1.45 Å, which represents the Fe bonding to the anion (O and F) in the discharged states [23,24,44,45], increases as cycling proceeds, which supports the idea that the primary electrochemical reaction shifts from a 'surface conversion' to a 'host formation' reaction as cycling progresses. After cycling, the signals for the charged and discharged samples in both the TEY and TFY modes were almost identical, indicating that the host structure formation was completed and it is well maintained during charge and discharge (Fig. S8).

The electrochemical responses before and after host formation were examined using CV, as shown in Fig. 5 (a) and (b). The CV tests were performed in the 2nd and 20th cycles at scan rates between 0.075 and 1 mV/s to distinctively investigate the behaviors before and after the host formation. Before the host formation (Fig. 5 (a)), both the anodic and cathodic peaks increased with increasing scan rate without a change in the peak position, which is a typical characteristic of a surface capacitive reaction [21]. However, as shown in Fig. 5 (b), in the 20th cycles (*i.e.,* after the host formation), both the anodic and cathodic peaks shifted with increasing scan rate, indicative of a diffusion-limited process, which is often observed in electrode reactions involving an intercalation process [46]. The rate capability results also clearly support the idea that the electrochemical responses of the electrodes changed as cycling progressed, as shown in Fig. 5 (c) and (d). The rate tests were performed by increasing the discharge current density from 50 to 2000 mA/g. Fig. 5 (c) shows that the capacity decrease and voltage drop at high current were relatively small before the host formation, which is attributed to the surface electrochemical reaction. Approximately 70% of the low-rate capacity (the capacity at 50 mA/g) was retained at the current density of 2000 mA/g. However, relatively smaller capacity retention could be achieved after the host formation, where 55% of the low-rate capacity (capacity at 50 mA/g) was maintained at the current density of 2000 mA/g. This result indicates the comparatively sluggish reaction of intercalation compared with the surface conversion reaction.

Inspired by the finding that the cubic FeOF host can also be formed

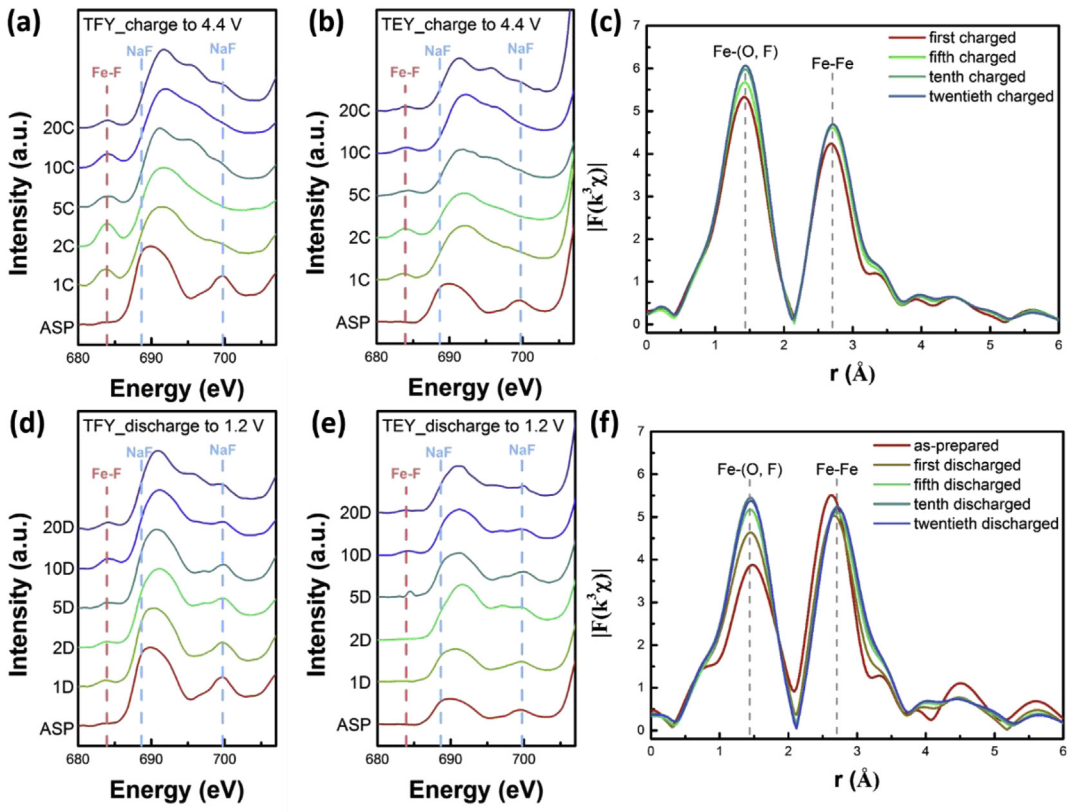

Fig. 4. *Ex situ* F K-edge XAS spectra measured in charged state in **(a)** TFY mode and **(b)** TEY mode. The number represents the cycle number, and C and D indicates the charged and discharged state, respectively. **(c)** The Fe K-edge EXAFS spectra measured in the charged state. F K-edge XAS results measured in the discharged state in **(d)** TFY mode and **(e)** TEY mode. **(f)** The Fe K-edge EXAFS spectra measured in the discharged state.

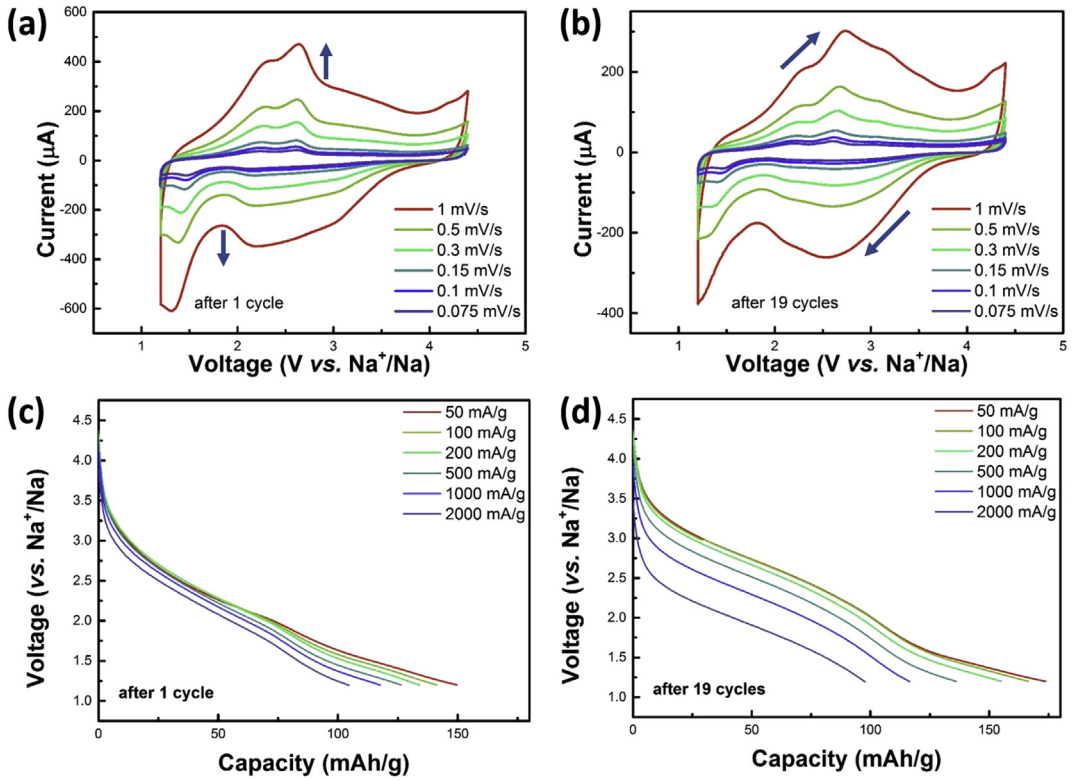

Fig. 5. CV profiles of NaF–FeO nanocomposite electrode at various scan rates after **(a)** 1 cycle and **(b)** 19 cycles. Discharge profiles at various discharge current densities after **(c)** 1 cycle and **(d)** 19 cycles.

from FeO serving as a Na-ion host in the Na electrochemical system, similar to the Li electrochemical system [22], we attempted to verify whether this phenomenon is universal for other alkali metal systems. A KF–FeO nanocomposite was synthesized using high-energy ball milling and tested in a K half-cell configuration. Fig. S9 shows that the KF–FeO nanocomposite electrode could deliver a first discharge capacity of 100 mAh/g with reversible Fe oxidation and reduction during the cycle. However, notably, the charge/discharge profile did not change, and capacity increase was not observed as cycling progressed (Fig. S10). This finding differed from the results for the LiF–FeO and NaF–FeO nanocomposites, where a profile change was observed during cycling, accompanying the host formation reaction. The CV curves of KF–FeO in the 2nd and 20th cycles were typical profiles of surface electrochemical reactions, where the peak position does not change with scan rate (Fig. S11). Both the charge/discharge profiles and CV results indicate that the host formation for K ions was not induced in the KF–FeO nanocomposite electrode during cell operation. In Fig. S12, it was observed that in the discharged state after 20 cycles, the majority of the peaks from the *ex situ* XRD analysis of the KF–FeO nanocomposite still corresponded to FeO while traces of cubic FeOF could be detected. These findings along with the results above suggest that the complete phase transformation from cubic FeO to cubic FeOF might be aided by an intercalation/deintercalation reaction of an alkali ion such as Li or Na. It is speculated that in the KF–FeO case, larger K ions may not be suitable for intercalation into the cubic FeOF structure, which would prohibit further transformation from FeO to cubic FeOF.

In summary, we investigated the Na storage behavior in a nanocomposite electrode of NaF and FeO in a Na electrochemical cell. *Ex situ* XRD and HAADF-STEM analysis revealed the formation of cubic FeOF, different from rutile FeOF, during cell operation of the NaF–FeO nanocomposite, which is analogous to previously reported results for a Li electrochemical cell. As the host structure is formed for Na-ion storage, the average voltage increases from 2.0 to 2.25 V, and the discharge capacity increases from 150 to 165 mAh/g. F K-edge XAS analysis and results for the KF–FeO nanocomposite suggest that the phase transformation of FeO to cubic FeOF occurs gradually as cycling progresses and that full transformation is only possible when the appropriate alkali ion sources are utilized. The work presented here broadens our understanding of the electrochemistry of nanocomposite electrodes and helps to open up new possibilities for finding promising electrode materials by screening polymorphs of pre-existing cathode materials.

Acknowledgements

This work was supported by Samsung Research Funding Centre of Samsung Electronics under project number SRFC-TA1403-52.

Appendix A. Supplementary data

Supplementary data to this article can be found online at https://doi.org/10.1016/j.ensm.2019.04.020.

References

[1] C. Delmas, Sodium and sodium-ion batteries: 50 Years of research, Adv. Energy Mater. (2018) 1703137.
[2] S.W. Kim, D.H. Seo, X. Ma, G. Ceder, K. Kang, Electrode materials for rechargeable sodium-ion batteries: potential alternatives to current lithium-ion batteries, Adv. Energy Mater. 2 (2012) 710–721.
[3] H. Kim, H. Kim, Z. Ding, M.H. Lee, K. Lim, G. Yoon, K. Kang, Recent progress in electrode materials for sodium-ion batteries, Adv. Energy Mater. 6 (2016) 1600943.
[4] V. Palomares, P. Serras, I. Villaluenga, K.B. Hueso, J. Carretero-González, T. Rojo, Na-ion batteries, recent advances and present challenges to become low cost energy storage systems, Energy Environ. Sci. 5 (2012) 5884–5901.
[5] C. Delmas, J.-J. Braconnier, C. Fouassier, P. Hagenmuller, Electrochemical intercalation of sodium in NaxCoO2 bronzes, Solid State Ionics 3 (1981) 165–169.
[6] X. Ma, H. Chen, G. Ceder, Electrochemical properties of monoclinic NaMnO2, J. Electrochem. Soc. 158 (2011) A1307–A1312.
[7] S. Komaba, C. Takei, T. Nakayama, A. Ogata, N. Yabuuchi, Electrochemical intercalation activity of layered NaCrO2 vs. LiCrO2, Electrochem. Commun. 12 (2010) 355–358.
[8] C.-Y. Yu, J.-S. Park, H.-G. Jung, K.-Y. Chung, D. Aurbach, Y.-K. Sun, S.-T. Myung, NaCrO 2 cathode for high-rate sodium-ion batteries, Energy Environ. Sci. 8 (2015) 2019–2026.
[9] S.-M. Oh, S.-T. Myung, C.S. Yoon, J. Lu, J. Hassoun, B. Scrosati, K. Amine, Y.-K. Sun, Advanced Na [Ni0. 25Fe0. 5Mn0. 25] O2/C–Fe3O4 sodium-ion batteries using EMS electrolyte for energy storage, Nano Lett. 14 (2014) 1620–1626.
[10] M.H. Han, E. Gonzalo, M. Casas-Cabanas, T. Rojo, Structural evolution and electrochemistry of monoclinic NaNiO2 upon the first cycling process, J. Power Sources 258 (2014) 266–271.
[11] A. Mendiboure, C. Delmas, P. Hagenmuller, Electrochemical intercalation and deintercalation of NaxMnO2 bronzes, J. Solid State Chem. 57 (1985) 323–331.
[12] W.K. Pang, S. Kalluri, V.K. Peterson, N. Sharma, J. Kimpton, B. Johannessen, H.K. Liu, S.X. Dou, Z. Guo, Interplay between electrochemistry and phase evolution of the P2-type Na x (Fe1/2Mn1/2) O2 cathode for use in sodium-ion batteries, Chem. Mater. 27 (2015) 3150–3158.
[13] N. Yabuuchi, M. Kajiyama, J. Iwatate, H. Nishikawa, S. Hitomi, R. Okuyama, R. Usui, Y. Yamada, S. Komaba, P2-type Na x [Fe 1/2 Mn 1/2] O 2 made from earth-abundant elements for rechargeable Na batteries, Nat. Mater. 11 (2012) 512.
[14] N. Yabuuchi, H. Yoshida, S. Komaba, Crystal structures and electrode performance of alpha-NaFeO2 for rechargeable sodium batteries, Electrochemistry 80 (2012) 716–719.
[15] M. Bianchini, F. Fauth, N. Brisset, F. Weill, E. Suard, C. Masquelier, L. Croguennec, Comprehensive investigation of the Na3V2 (PO4) 2F3–NaV2 (PO4) 2F3 system by operando high resolution synchrotron X-ray diffraction, Chem. Mater. 27 (2015) 3009–3020.
[16] Y.U. Park, D.H. Seo, H. Kim, J. Kim, S. Lee, B. Kim, K. Kang, A family of high-performance cathode materials for Na-ion batteries, Na3 (VO1− xPO4) 2 F1+ 2x (0≤ x≤ 1): combined first-principles and experimental study, Adv. Funct. Mater. 24 (2014) 4603–4614.
[17] Z. Jian, W. Han, X. Lu, H. Yang, Y.S. Hu, J. Zhou, Z. Zhou, J. Li, W. Chen, D. Chen, Superior electrochemical performance and storage mechanism of Na3V2 (PO4) 3 cathode for room-temperature sodium-ion batteries, Adv. Energy Mater. 3 (2013) 156–160.
[18] P. Barpanda, M. Ati, B.C. Melot, G. Rousse, J.-N. Chotard, M.-L. Doublet, M.T. Sougrati, S. Corr, J.-C. Jumas, J.-M. Tarascon, A 3.90 V iron-based fluorosulphate material for lithium-ion batteries crystallizing in the triplite structure, Nat. Mater. 10 (2011) 772.
[19] N. Recham, J.-N. Chotard, L. Dupont, C. Delacourt, W. Walker, M. Armand, J.-M. Tarascon, A 3.6 V lithium-based fluorosulphate insertion positive electrode for lithium-ion batteries, Nat. Mater. 9 (2010) 68.
[20] R. Tripathi, G.R. Gardiner, M.S. Islam, L.F. Nazar, Alkali-ion conduction paths in LiFeSO4F and NaFeSO4F tavorite-type cathode materials, Chem. Mater. 23 (2011) 2278–2284.
[21] S.-K. Jung, H. Kim, M.G. Cho, S.-P. Cho, B. Lee, H. Kim, Y.-U. Park, J. Hong, K.-Y. Park, G. Yoon, Lithium-free transition metal monoxides for positive electrodes in lithium-ion batteries, Nat. Energy 2 (2017) 16208.
[22] S.-K. Jung, I. Hwang, S.-P. Cho, K. Oh, K. Ku, I.R. Choi, K. Kang, New iron-based intercalation host for lithium-ion batteries, Chem. Mater. 30 (2018) 1956–1964.
[23] S.-W. Kim, K.-W. Nam, D.-H. Seo, J. Hong, H. Kim, H. Gwon, K. Kang, Energy storage in composites of a redox couple host and a lithium ion host, Nano Today 7 (2012) 168–173.
[24] I. Hwang, S.-K. Jung, E.-S. Jeong, H. Kim, S.-P. Cho, K. Ku, H. Kim, W.-S. Yoon, K. Kang, NaF–FeF 2 nanocomposite: new type of Na-ion battery cathode material, Nano Res. 10 (2017) 4388–4397.
[25] N. Dimov, A. Kitajou, H. Hori, E. Kobayashi, S. Okada, Electrochemical splitting of LiF: a new approach to lithium-ion battery materials, ECS Trans. 58 (2014) 87–99.
[26] L. Zhang, G. Chen, E.J. Berg, J.M. Tarascon, Triggering the in situ electrochemical formation of high capacity cathode material from MnO, Adv. Energy Mater. 7 (2017).
[27] L. Zhang, D. Batuk, G. Chen, J.-M. Tarascon, Electrochemically activated MnO as a cathode material for sodium-ion batteries, Electrochem. Commun. 77 (2017) 81–84.
[28] R. Kataoka, M. Kitta, N. Takeichi, T. Kiyobayashi, Electrochemical in situ synthesis: a new synthesis route for redox active manganese oxides for rechargeable sodium ion battery through initial charge process, J. Electrochem. Soc. 164 (2017) A226–A230.
[29] A. Kitajou, J. Arai, S. Okada, in: Cathode Properties of Amorphous Xllif-FeSO4 (x= 1.0, 1.2 and 1.5) Composite for Li-Ion Batteries, Meeting Abstracts, The Electrochemical Society, 2016, 258-258.
[30] A. Kitajou, E. Kobayashi, S. Okada, Electrochemical performance of a novel cathode material "LiFeOF" for Li-ion batteries, Electrochemistry 83 (2015) 885–888.
[31] S. Okada, D. Tsunoe, A. Kitajou, H. Hori, N. Dimov, P. Barpanda, in: Possibility of Composite Cathodes with Sacrificial Salts, Meeting Abstracts, 2016; the Electrochemical Society, 2016, 33-33.
[32] L. Fu, K. Tang, H. Oh, K. Manickam, T. Bräuniger, C.V. Chandran, A. Menzel, M. Hirscher, D. Samuelis, J. Maier, "Job-Sharing" storage of hydrogen in Ru/Li2O nanocomposites, Nano Lett. 15 (2015) 4170–4175.
[33] C.-C. Chen, J. Maier, Decoupling electron and ion storage and the path from interfacial storage to artificial electrodes, Nat. Energy 3 (2018) 102.
[34] S.-i. Nakai, M. Ohashi, T. Mitsuishi, H. Maezawa, H. Oizumi, T. Fujikawa, F–K XANES studies of alkali fluorides, J. Phys. Soc. Jpn. 55 (1986) 2436–2442.
[35] Y. Shao, H. Yue, R. Qiao, J. Hu, G. Zhong, S. Wu, M.J. McDonald, Z. Gong, Z. Zhu, W. Yang, Synthesis and reaction mechanism of novel fluorinated carbon fiber as a

high-voltage cathode material for rechargeable Na batteries, Chem. Mater. 28 (2016) 1026–1033.
[36] E. Hudson, E. Moler, Y. Zheng, S. Kellar, P. Heimann, Z. Hussain, D. Shirley, Near-edge sodium and fluorine K-shell photoabsorption of alkali halides, Phys. Rev. B 49 (1994) 3701.
[37] F. Cosandey, J.F. Al-Sharab, F. Badway, G.G. Amatucci, P. Stadelmann, EELS spectroscopy of iron fluorides and FeF x/C nanocomposite electrodes used in Li-ion batteries, Microsc. Microanal. 13 (2007) 87–95.
[38] S. Nakai, A. Kawata, M. Ohashi, M. Kitamura, C. Sugiura, T. Mitsuishi, H. Maezawa, Core-exciton absorption in the F K absorption spectra of 3d transition-metal fluorides, Phys. Rev. B 37 (1988) 10895.
[39] M. Saifullah, G. Botton, C. Boothroyd, C. Humphreys, Electron energy loss spectroscopy studies of the amorphous to crystalline transition in FeF 3, J. Appl. Phys. 86 (1999) 2499–2504.
[40] Y.N. Zhou, M. Sina, N. Pereira, X. Yu, G.G. Amatucci, X.Q. Yang, F. Cosandey, K.W. Nam, FeO0. 7F1. 3/C nanocomposite as a high-capacity cathode material for sodium-ion batteries, Adv. Funct. Mater. 25 (2015) 696–703.
[41] S.Y. Fu, Y.Z. Li, W. Chu, Y.M. Yang, D.G. Tong, Q. Le Zeng, Mesoporous amorphous FeOF nanococoons for high-rate and long-life rechargeable sodium-ion batteries, J. Mater. Chem. 3 (2015) 16716–16727.
[42] J. Zhu, D. Deng, Wet-chemical synthesis of phase-pure FeOF nanorods as high-capacity cathodes for sodium-ion batteries, Angew. Chem. Int. Ed. 54 (2015) 3079–3083.
[43] N. Pereira, F. Badway, M. Wartelsky, S. Gunn, G. Amatucci, Iron oxyfluorides as high capacity cathode materials for lithium batteries, J. Electrochem. Soc. 156 (2009) A407–A416.
[44] A. Kuzmin, P. Parent, Focusing and superfocusing effects in X-ray absorption fine structure at the iron K edge in FeF3, J. Phys. Condens. Matter 6 (1994) 4395.
[45] F. Wang, S.-W. Kim, D.-H. Seo, K. Kang, L. Wang, D. Su, J.J. Vajo, J. Wang, J. Graetz, Ternary metal fluorides as high-energy cathodes with low cycling hysteresis, Nat. Commun. 6 (2015) 6668.
[46] Y. Denis, C. Fietzek, W. Weydanz, K. Donoue, T. Inoue, H. Kurokawa, S. Fujitani, Study of LiFePO4 by cyclic voltammetry, J. Electrochem. Soc. 154 (2007) A253–A257.